Plant Cell Rep
DOI 10.1007/s00299-015-1860-3

ORIGINAL ARTICLE

Identification of geranylgeranyl diphosphate synthase genes from *Tripterygium wilfordii*

Meng Zhang[1] · Ping Su[1,2] · Yong-Jin Zhou[3] · Xiu-Juan Wang[1] · Yu-Jun Zhao[2] · Yu-Jia Liu[1] · Yu-Ru Tong[1,2] · Tian-Yuan Hu[1] · Lu-Qi Huang[2] · Wei Gao[1]

Received: 6 June 2015 / Revised: 27 August 2015 / Accepted: 31 August 2015

Abstract

Key message **We found triptolide synthesis is correlated with the expressions of *TwGGPPS1* and *TwGGPPS4*. This lays the foundation for future studies of biosynthetic pathways for triptolide and other diterpenoids in *T. wilfordii*.**

Abstract *Tripterygium wilfordii* is a traditional Chinese medical plant commonly used to treat rheumatoid arthritis. One of its main bioactive compounds is triptolide, which is identified as an abietane-type diterpenoid natural product. Geranylgeranyl diphosphate synthase (GGPPS) catalyses the synthesis of GGPP (geranylgeranyl diphosphate), the common precursor of diterpenes, and is therefore a crucial enzyme in diterpene biosynthesis. A previous study showed that GGPP could be catalyzed by copalyl diphosphate synthase and kaurene synthase like of *Salvia miltiorrhiza* (SmCPS, SmKSL) to miltiradiene, a key intermediate in tanshinone biosynthesis. In this paper, five new full-length cDNAs (*TwGGPPS*) encoding GGPP synthases were cloned from *T. wilfordii*. Sequence comparisons revealed that all six *TwGGPPSs* (including *TwGGPPS2* cloned previously) exhibit similarities to *GGPPSs* of other plants. Subsequent functional complement assays demonstrated that TwGGPPS1, TwGGPPS4 and TwGGPPS5 can participate in miltiradiene biosynthesis in the recombinant *E. coli*. Correlation analysis of gene expressions and secondary metabolite accumulation indicated that TwGGPPS1 and TwGGPPS4 are likely involved in the biosynthesis of triptolide. These findings lay the foundation for future studies of the biosynthetic pathways for triptolide and other diterpenoids in *T. wilfordii*.

Keywords GGPPS · *Tripterygium wilfordii* · Triptolide · Biosynthesis

Communicated by B. Li.

M. Zhang and P. Su contributed equally to this work.

Electronic supplementary material The online version of this article (doi:10.1007/s00299-015-1860-3) contains supplementary material, which is available to authorized users.

✉ Xiu-Juan Wang
wxj0517@sina.com

✉ Lu-Qi Huang
huangluqi01@126.com

✉ Wei Gao
weigao@ccmu.edu.cn

Meng Zhang
zhangmeng8846@163.com

[1] School of Traditional Chinese Medicine, Capital Medical University, Beijing 100069, China

[2] National Resource Center for Chinese Materia Medica, China Academy of Chinese Medical Sciences, Beijing 100700, China

[3] Department of Chemical and Biological Engineering, Chalmers University of Technology, Kemivägen 10, 41296 Göteborg, Sweden

Introduction

Tripterygium wilfordii is a traditional Chinese medical plant commonly used in the treatment of rheumatoid arthritis (Liu et al. 2013), nephrotic syndrome (Jiang 1994), systemic lupus erythematosus (Patavino and Brady 2001). And more than 380 secondary metabolites have been reported from *Tripterygium* species, including terpenoids, alkaloids, anthraquinones and so on (Brinker et al. 2007).

Published online: 08 October 2015

Biochemical analysis has shown that most of these natural products with strong biological activities, such as anticancer (Titov et al. 2011; Yang et al. 2003; Kannaiyan et al. 2011), immunosuppressive (Liu et al. 2005) and anti-inflammatory (Li et al. 2008). Because of the variety of activities, *T. wilfordii* is increasingly used in the clinical treatment and has attracted wide attention of researchers around the world. Among the secondary metabolites from *T. wilfordii*, triptolide, the diterpenoid compound, is thought to be the major active component. And most of the anti-inflammatory and immunosuppressive activities of extracts can be attributed to triptolide (Brinker et al. 2007), which may also represent an important active molecule for the treatment of Parkinson's and Alzheimer's disease (Wang et al. 2008; Li et al. 2010; Ren et al. 2010). In addition, a recent study suggests that triptolide has therapeutic potential for bone lytic diseases caused by prosthetic wear particle (Huang et al. 2015). Therefore, it is important to elucidate the triptolide biosynthesis pathway in *T. wilfordii* plant.

In general, diterpenoid biosynthesis pathways in plants can be divided into three phases. The first phase involves the synthesis of isopentenyl pyrophosphate (IPP) and its isomer, dimethylallyl pyrophosphate (DMAPP). Two terpenoid backbone biosynthesis pathways are known in this phase: the cytosolic mevalonic acid (MVA) pathway (Newman and Chappell 1999) and the plastidial 2-methyl-D-erythritol-4-phosphate (MEP) pathway (Rohmer et al. 1993). There is crosstalk between them via isoprenoid intermediates (Laule et al. 2003). In the second phase, geranylgeranyl diphosphate synthase (GGPPS) catalyses the successive addition of IPP to dimethylallyl pyrophosphate (DMAPP), geranyl pyrophosphate (GPP) and farnesyl pyrophosphate (FPP) to form GGPP (Vandermoten et al. 2009). In the last phase, GGPP is catalyzed by diterpene synthases (diTPS) to form various intermediates (Gao et al. 2009), which are then modified by related enzymes to create specific diterpenoid end products (Fig. 1) (Zhao et al. 2014).

Triptolide is an abietane-type diterpenoid natural product and shares many similarities with tanshinones, the bioactive components found in the Chinese medicinal herb *Salvia miltiorrhiza*. A series of studies have revealed the components of the tanshinone biosynthesis pathway, in which two types of diTPSs, SmCPS and SmKSL, transform GGPP in a stepwise fashion into miltiradiene, the key intermediate of tanshinones (Fig. 1) (Gao et al. 2009). In more recent studies, the active sites of these two diTPSs were engineered using protein fusions to bring them into close proximity to enhance metabolic flux channeling and miltiradiene biosynthesis. This fusion protein yields significantly increased miltiradiene production and reduced byproduct accumulation in the engineered yeast strain YJ26 (Zhou et al. 2012).

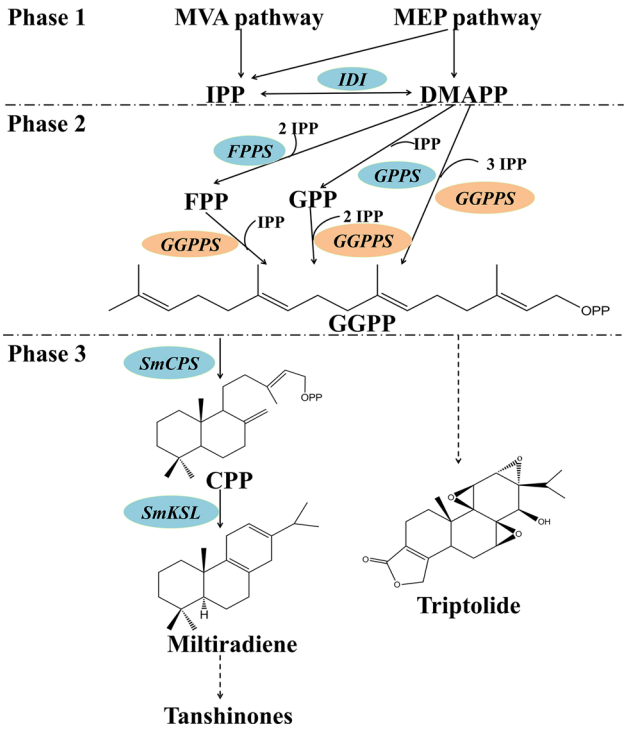

Fig. 1 Biosynthetic pathway of diterpenoids. *Each solid arrow* represents a biosynthetic reaction step, and *dashed arrows* represent multiple-step reactions. *IDI* isopentenyl-diphosphate delta-isomerase, *CPP* copalyl diphosphate

At present, the triptolide biosynthesis pathway is not well known. However, triptolide does share some pathways with the diterpenoids. As the essential acyclic precursor, GGPP is the common precursor for diterpenoids, including carotenoids, chlorophylls, ubiquinones and other diterpenes. Therefore, GGPPS is considered to be one of the key synthases in the diterpenoid biosynthesis pathway. Indeed, the identification of this enzyme has significant implications for the study of triptolide biosynthesis in *T. wilfordii*. Although *GGPPS* genes have been cloned from many plants, there are no reports describing GGPPS in *T. wilfordii*. For the first time, we report the cloning of five new full-length GGPPS cDNAs from *T. wilfordii* (*TwGGPPSs*), and we characterized them using a miltiradiene metabolic engineering approach in *E. coli*. In addition, we analyzed the expression of these new genes and monitored the production of triptolide in *T. wilfordii* cell suspensions following induction with methyl jasmonate (MeJA), revealing that two GGPPS genes are involved in the biosynthesis of triptolide.

Materials and methods

Plant material and growth conditions

The *T. wilfordii* cell suspensions were cultured in Murashige and Skoog (MS) medium containing 30 g/L sucrose with 0.1 mg/L kinetin (KT), 0.5 mg/L indole-3-butyric acid (IBA) and 0.5 mg/L 2,4-dichlorophenoxyacetic acid (2,4-D). All cell suspensions were maintained at 25 ± 1 °C with 120 rpm shaking in the dark.

RNA isolation and cDNA synthesis

Total RNA was isolated using the cetyltrimethylammonium bromide (CTAB) method (Del Sal et al. 1989). The total RNA was treated with RNA Purification Kit (Tiangen Biotech, Beijing, China) to remove genomic DNA and obtain purified RNA. The 3′- or 5′-RACE-ready cDNA was reverse transcribed from the purified RNA using the SMARTer^{TM} RACE cDNA Amplification Kit (Clontech Laboratories, Cal., USA). First-stand cDNA for real-time quantitative PCR was reverse transcribed from total RNA using the FastQuant RT Kit (Tiangen Biotech, Beijing, China).

Rapid amplification of cDNA ends

Five putative GGPPS fragments were identified by analyzing a previously obtained *T. wilfordii* transcriptome sequencing dataset. The SMARTer^{TM} RACE cDNA Amplification Kit was used to amplify the 3′ and 5′ ends of the five *TwGGPPS* cDNAs. The 3′ (G-3) and 5′ (G-5) gene-specific primers were designed based on these fragments (Table S1). 3′ RACE amplification was performed using primer G-3 and Universal Primer A Mix (UPM, provided in the kit) with the 3′-RACE ready cDNA as a template. 5′ RACE amplification was performed using the G-5 primer and UPM with the 5′-RACE-ready cDNA as a template. All the reactions were performed according to the user's manual. The products were purified and cloned into the pMD19-T vector (Takara Biotechnology, Dalian, China), transformed into *E. coli* DH5α cells, and then cultured in Luria–Bertani medium at 37 °C in the dark. Positive colonies were sequenced.

Cloning of the *TwGGPPS* full-length cDNA

Primers to amplify the full-length cDNAs (G-F and G-R) were designed based on the assembled core fragments of the 3′ and 5′ RACE sequences (Table S1). The amplification reactions were performed using PrimeSTAR GXL DNA Polymerase (Takara Biotechnology, Dalian, China), according to the manufacturer's instructions. The products were purified and cloned into the pMD19-T vector, transformed into *E. coli* DH5α cells, and then sequenced.

Bioinformatics analysis

The open reading frames for the *TwGGPPSs* were deduced using the online tool ORF Finder (http://www.ncbi.nlm.nih.gov/gorf/gorf.html). The ExPASy online tool (http://web.expasy.org/compute_pi/) was used to calculate the isoelectric point (pI) and relative molecular weight (Mw) of the putative protein. Interpro (www.ebi.ac.uk/Tools/InterProScan) was used to identify functional domains. The TargetP 1.1 server (http://www.cbs.dtu.dk/services/TargetP/) and PSORT (http://psort.hgc.jp/) algorithms were used to predict signal peptides and subcellular localisation. The sequences of the TwGGPPSs as well as other GGPPS sequences downloaded from GenBank were aligned using the DNAMAN program, and the phylogenetic tree was constructed using MEGA 4 software.

Functional identification

In this study, the coding regions of *TwGGPPS* and *SmCPS/KSL* were cloned into the expression vector pETDuet-1 to construct a miltiradiene biosynthetic pathway in *E. coli* (Fig. 2A).

Construction of recombinant E. coli BL21 strains

The *TwGGPPS* ORF was amplified using the primers OG-F and OG-R (Table S1). The *TwGGPPS* amplification products were then digested using the following restriction enzymes (Takara Biotechnology, Dalian, China): *TwGGPPS1* with *Sal*I and *Afl*II; *TwGGPPS3* and *TwGGPPS6* with *Hind*III and *EcoR*I; and *TwGGPPS2, TwGGPPS4* and *TwGGPPS5* with *BamH*I and *Sal*I. Next, the PCR fragments were inserted into pETDuet-1 vectors that had been digested with the same restriction enzymes, yielding six distinct pEG vectors. Then, the primer pair CK-F and CK-R (Table S1) was used to amplify the fusion gene fragment *SmCPS/KSL* from the plasmid YJ26 (Zhou et al. 2012), which was then digested with *Nde*I and *Kpn*I. The six pEG vectors as well as pETDuet-1 were also digested with *Nde*I and *Kpn*I, and the *Nde*I-*Kpn*I *SmCPS/KSL* fragment was ligated into each vector to yield six pEG-CK plasmids as well as the plasmid pET-CK, which was used as a negative control (Fig. 2B). All seven plasmids were sequenced to verify the correct insertions.

E. coli BL21(DE3) cells were transformed with the six pEG-CK plasmids and pET-CK and cultured on solid LB medium containing 100 mg/L ampicillin. Positive colonies were selected and grown in liquid LB medium at 250 rpm at 37 °C overnight and then incubated at 30 °C for an additional day.

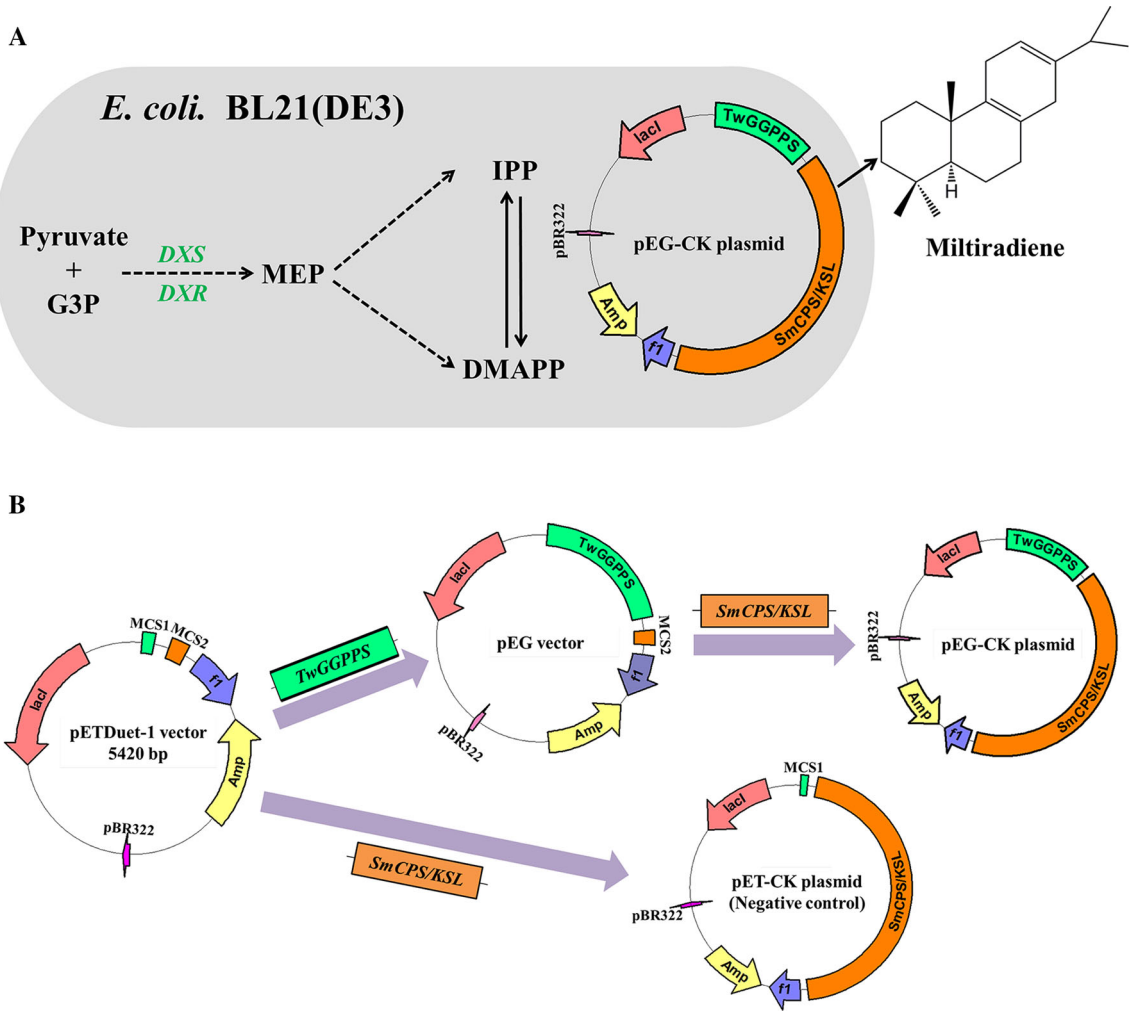

Fig. 2 Function assay in *E. coli*. **A** MEP pathway is occurred in *E. coli* BL21(DE3). Biosynthetic pathway of miltiradiene was built in it. G3P:glyceraldehyde-3-phosphate. *DXS* 1-deoxy-D-xylulose-5-phosphate synthase, *DXR* 1-deoxy-D-xylulose-5-phosphate reductoisomerase. **B** The process of plasmid construction used in *E. coli*

GC–MS analysis

In total, 250 mL of the bacterial solution was centrifuged at 8000 rpm for 5 min to separate the bacterial pellet from the culture medium. Bacterial pellets were resuspended in 10 mL phosphate buffered saline (PBS, pH 7.0) and then lysed by a sonicator with 6 times 10-s burst and 10-s interval. Next, the PBS containing the disrupted bacterial pellet was extracted with 30 mL *n*-hexane 3 times. The culture medium was extracted with the same volume of *n*-hexane 3 times. The two extracts were then combined, evaporated under N_2, and dissolved in 500 µL *n*-hexane for the GC–MS measurements. And the miltiradiene standard sample prepared by our team previous was detected by GC–MS as a positive control. GC–MS analysis was performed on a Thermo TRACE 1310/TSQ 8000 gas chromatograph (splitless; injector temperature, 250 °C) with a DB-5 ms (30 m × 0.25 mm × 0.25 µm) capillary column. One microlitre of the concentrated organic phase was then injected under an He flow rate of 1 mL/min with a temperature program of 2 min at 50 °C, followed by a gradient from 50 to 300 °C at 20 °C/min with a 20 min hold at 300 °C. The ion trap heating temperature was 250 °C. The electron energy was 70 eV. Spectra were recorded in the range of 50–450 m/z.

Methyl jasmonate induction

After the *T. wilfordii* suspension cells had been cultivated for 10 days, cells in induced group were treated with methyl jasmonate (MeJA) in carrier solution (dimethyl sulfoxide) at the final concentration of 50 µM. Cells in control group were only treated with same volume of carrier solution. Subsequently, the cells were harvested for RNA isolation at 0, 4, 12, 48, 72 h. Three samples were prepared for each time point in each group.

Table 1 Information of six full-length *TwGGPPS* cDNAs

	TwGGPPS1	*TwGGPPS2*	*TwGGPPS3*	*TwGGPPS4*	*TwGGPPS5*	*TwGGPPS6*
The basic information of nucleotide sequence						
GenBank ID	KM978332	KM978333	KP010363	KP010364	KP010365	KP010366
Full-length	1666 bp	1857 bp	1329 bp	1400 bp	1291 bp	1282 bp
ORF	384–1469 bp	27–1571 bp	16–1062 bp	120–1070 bp	126–1151 bp	73–1023 bp
The information of predicted protein						
Amino Acid	361	514	348	316	341	316
Mw	39.40 kD	57.13 kD	38.27 kD	34.38 kD	37.13 kD	34.46 kD
pI	8.14	7.85	5.61	5.51	6.27	6.64
Functional region	FARM, SARM	FARM, SARM	FARM	FARM, SARM	FARM, SARM	–
Conserved domain	I–V	I–V	II	II–V	I–V	–
Subcellular localisation	Chloroplast	Plasma membrane	Chloroplast	Cytoplasm	Plasma membrane	Chloroplast
Resource	This study	Zhang et al. (2015)	This study	This study	This study	This study

The basic information about nucleotide sequences and their predicted proteins were analyzed. Functional regions, conserved domains and localization were predicted as well

Quantitative real-time PCR was performed using an Applied Biosystems 7300 Real-Time PCR System (Applied Biosystems, New York, USA) with the KAPA SYBR® FAST qPCR Kit (KAPA Biosystems, Massachusetts, USA) to estimate the relative mRNA expression levels. β-actin, a housekeeping gene, was used to normalize the expression levels of the target genes. The expression of *TwGGPPS* was evaluated using the $2^{-\Delta\Delta Ct}$ method (Livak and Schmittgen 2001). All primers used in the quantitative real-time PCR analyses are shown in Table S1. Each sample was amplified three times to ensure data reliability.

Phytochemical analysis

The same *T. wilfordii* cell suspensions used for the *TwGGPPS* expression analyses were harvested at 0, 4, 12, 48, 72, 120, 240 h for HPLC analysis. The harvested cell suspensions were frozen at −80 °C and then freeze-dried for 8 h. The samples were then prepared according to a previously reported method (Su et al. 2014). Analyses were performed using an Agilent 1260 HPLC system (USA) with an Agilent Eclipse XDB-C18 analytical column (5 μm, 4.6 × 250 mm; Agilent, USA). The mobile phase consisting of water (A) and acetonitrile (B) was set at a flow rate of 0.8 mL/min. The samples were then eluted with 38 % (B) for 12 min. The detection wavelength was 210 nm. The injection volume was 10 μL.

Results and discussion

Cloning of *TwGGPPS* full-length cDNA

Five putative full-length *TwGGPPS* cDNAs were obtained and registered in GenBank (Table 1). The results of the RACE and full-length PCR amplifications are shown in Fig. S1. Blast results showed that these six *TwGGPPS* genes (including *TwGGPPS2* cloned previously, Zhang et al. 2015) were similar to the known corresponding genes from other plants. *TwGGPPS1* shared 81 and 78 % identity with the *Lupinus albus* (AAA86688) and *Panax notoginseng* (AIK21792) GGPPS genes, respectively. *TwGGPPS2* shared 71 % identity with the *Theobroma cacao* (XP_007033017) GGPPS gene (Zhang et al. 2015). *TwGGPPS3* shared 81 % identity with a GGPPS gene from *Hevea brasiliensis* (BAF98303). *TwGGPPS4* and *TwGGPPS5* shared 71 and 69 % identities with the corresponding gene from *Populus trichocarpa* (XP_006383335), respectively. By contrast *TwGGPPS6* exhibited less than 60 % identity with the GGPPS genes from other plants.

GGPPS catalyses the successive addition of IPP to DMAPP, GPP and FPP to form GGPP (Vandermoten et al. 2009), and it belongs to the subfamily of short-chain isoprenyl diphosphate synthases. This enzyme shows a highly conserved structure with two aspartate-rich motifs, namely FARM (first aspartate-rich motif) and SARM (second aspartate-rich motif), which act as binding sites for allylic substrates and IPP, respectively (Hemmi et al. 2003). These motifs are thought to be important for GGPP synthase catalytic activity (Ashby et al. 1992; Joly and Edward 1993; Song and Poulter 1994). Product chain length is primarily governed by amino acid residues located at the fourth and fifth positions upstream of the FARM. Therefore, the upstream region and the FARM together make up the chain length determination domain (CLD). Based on CLD sequences, GGPPSs can be grouped into three types (Bouvier et al. 2005). In particular, plant GGPPSs are type II GGPP synthases, and they have four amino acid residues inserted in the FARM and are devoid of two aromatic

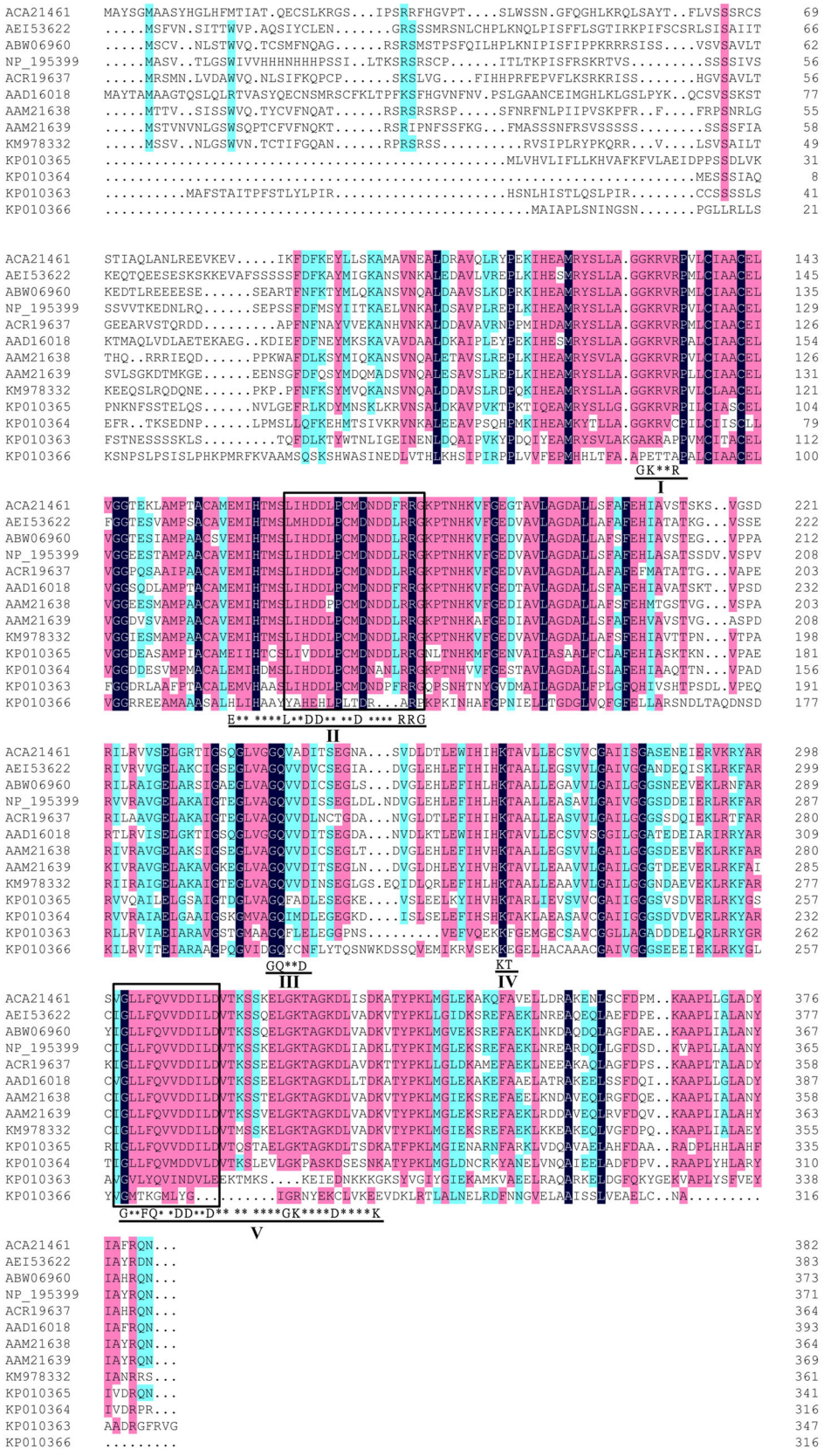

Fig. 3 Alignment of *TwGGPPS* with other GGPPS genes in plants. *I–V* represent five conserved domains, the *box* represents the two polyprenyl synthases functional regions. *Picea abies* (ACA21461), *Catharanthus roseus* (AEI53622), *Corylus avellana* (ABW06960), *Arabidopsis thaliana* GGPPS1(NP_195399), *Salvia miltiorrhiza* (ACR19637), *Taxus canadensis* (AAD16018), *Cistus creticus* (AAM21638), *Cistus creticus* (AAM21639), *TwGGPPS1* (KM978332), *TwGGPPS2* (KM978333), *TwGGPPS3* (KP010363), *TwGGPPS4* (KP010364), *TwGGPPS5* (KP010365), *TwGGPPS6* (KP010366)

amino acid residues at the fourth and fifth positions upstream of the FARM.

In this study, the multiple alignment with eight GGPPS amino acid sequences from other plants combined with Interpro analysis demonstrated that TwGGPPS1, TwGGPPS2, TwGGPPS4 and TwGGPPS5 possess the two characteristic GGPPS functional regions, FARM (DDXXXXD) and SARM (DDXXD), and therefore belong to the type II GGPP synthase subfamily, similar to the enzymes from other higher plants. TwGGPPS3 possesses only conserved domain II and a FARM functional region, whereas TwGGPPS6 possesses none of these domains (Table 1; Fig. 3). A phylogenetic tree was constructed using the six deduced amino acid sequences of the *TwGGPPS* genes as well as GGPPS sequences from other species (Fig. 4). This tree revealed that TwGGPPS1, TwGGPPS2, TwGGPPS4 and TwGGPPS5 clustered with the GGPP synthases in plant. TwGGPPS2 and TwGGPPS5 clustered and they were close to TwGGPPS4. TwGGPPS1 was more distantly related and clustered with GGPPS from *Theobroma cacao*. Although TwGGPPS3 and TwGGPPS6 did not cluster with the GGPPS sequences from plants, animals and other species, TwGGPPS3 was closer to them than TwGGPPS6. These findings suggest that the proteins encoded by *TwGGPPS3* and *TwGGPPS6* do not possess GGPP synthase activity.

A research found that a geranylgeranyl reductase (GGR; At4g38460) in *Arabidopsis* should be classified as class II small subunit (SSU), which lacks GGPPS activity because of its lacking the second conserved DDXXD motif, possesses 2 conserved CXXXC motifs and its gene is phylogenetically distinct from other *GGPPS*-like genes in *Arabidopsis* (Wang and Dixon 2009). In this study, TwGGPPS3 is similar to AtGGR. It might belong to SSU.

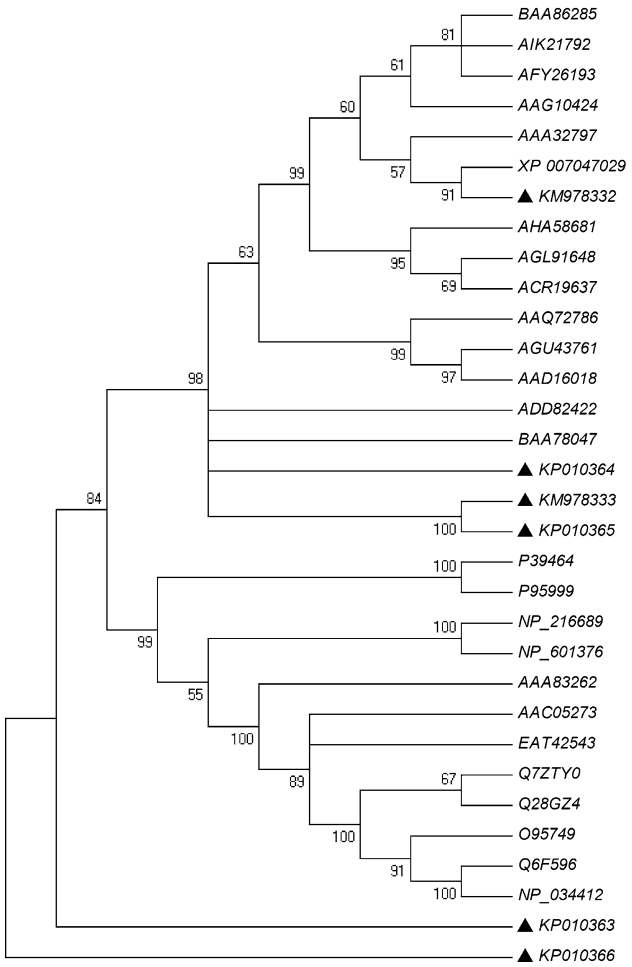

Fig. 4 Phylogenetic tree of GGPPS from different species. The tree was established with Neighbor-Joining method and cut-off value was 50 % for condensed tree. *Scoparia dulcis* (BAA86285), *Panax notoginseng* (AIK21792), *Picrorhiza kurroa* (AFY26193), *Tagetes erecta* (AAG10424), *Arabidopsis thaliana* (AAA32797), *Theobroma cacao* GGPPS1 (XP 007047029), *Nicotiana tabacum* GGPPS1 (AHA58681), *Catharanthus roseus* (AGL91648), *Salvia miltiorrhiza* (ACR19637), *Ginkgo biloba* (AAQ72786), *Pinus massoniana* (AGU43761), *Taxus Canadensis* (AAD16018), *Jatropha curcas* (ADD82422), *Daucus carota* (BAA78047), *Sulfolobus acidocaldarius* (P39464), *Sulfolobus solfataricus* (P95999), *Mycobacterium tuberculosis* H37RV (NP_216689), *Corynebacterium glutamicum* (NP_601376), *Saccharomyces cerevisiae* (AAA83262), *Drosophila melanogaster* (AAC05273), *Aedes aegypti* (EAT42543), *Danio rerio* (Q7ZTY0), *Xenopus tropicalis* (Q28GZ4), *Homo sapiens* (O95749), *Rattus norvegicus* (Q6F596), *Mus musculus* (NP_034412), *TwGGPPS1* (KM978332), *TwGGPPS2* (KM978333), *TwGGPPS3* (KP010363), *TwGGPPS4* (KP010364), *TwGGPPS5* (KP010365), *TwGGPPS6* (KP010366)

Functional identification in *E. coli*

The *TwGGPPS* genes were cloned into the pETDuet-1 vector together with *SmCPS/KSL* and then transformed into *E. coli* BL21(DE3). Functional GGPPS enzymes can catalyze the DMAPP and IPP present in *E. coli* to form GGPP, which can then be subsequently catalyzed by the fusion protein SmCPS/KSL to produce miltiradiene (Fig. 2A). Therefore, if miltiradiene is detected, this indicates that the corresponding *TwGGPPS* encodes a functional enzyme. The GC retention time (RT) of miltiradiene was 13.05 min; the extractions of recombinant BL21(DE3) strains containing pEG1-CK, pEG4-CK and pEG5-CK were detected compound (a) at 13.05 min. By contrast, the negative control, pEG2-CK, pEG3-CK and pEG6-CK samples were not detected compound (a). Meanwhile, as to pEG5-CK sample, there is another notable peak, compound (b), next to (a) (Fig. 5A). Under GC–MS analysis (Fig. 5B), the pEG1-CK, pEG4-CK and pEG5-CK sample products qualified as miltiradiene, which had the characteristic peaks, including m/z = 272.3 (molecular ion: M+), $m/z = 148.2$ and $m/z = 134.2$ (Gao et al. 2009). Compound (b) might be octasiloxane according to reference spectrum from NIST mass spectrum database (Fig. 5D). Therefore,

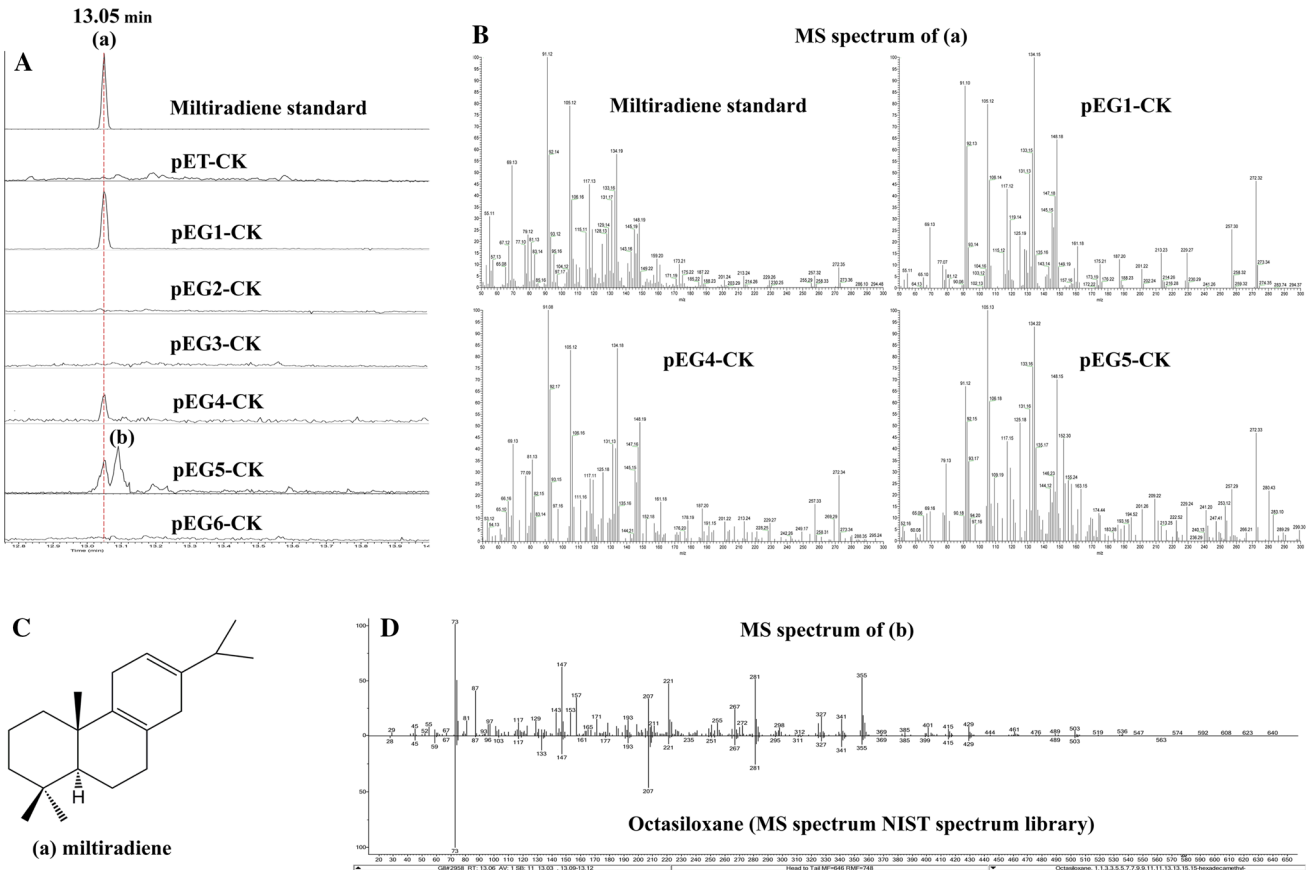

Fig. 5 Results of GC–MS. **A** A peak of compound (*a*) at 13.05 min occurred in miltiradiene standard and recombinant BL21(DE3) containing pEG1-CK, pEG4-CK and pEG5-CK, respectively. And there was a compound (*b*) next to (*a*) in pEG5-CK sample. **B** The MS results showed that the primary ion peaks of (*a*) belonged to miltiradiene. **C** The structure of miltiradiene. **D** The mass spectrum of (*b*) implied that it might be octasiloxane according to reference spectrum from NIST mass spectrum database

TwGGPPS1, *TwGGPPS4*, and *TwGGPPS5* encode the proteins that possess the activity of GGPP synthase.

Methyl jasmonate induction

To determine whether the three functional TwGGPPSs are involved in triptolide synthesis, we analyzed the expressions of the three functional genes as well as the accumulation of triptolide in cell suspensions induced with the plant defence signaling molecule MeJA, which is thought to be a general inducer of plant secondary metabolite biosynthesis (Memelink et al. 2001).

In the induced group, the relative expression level of *TwGGPPS1* reached the highest level at 4 h (12.8-fold that in the control group, Fig. S2), and the relative expression level of *TwGGPPS4* was increased at 4 and 12 h after MeJA treatment and the fold change was 2.3 and 2.5, respectively. The statistical analysis showed significant difference ($p < 0.01$) (Fig. S3). Compared with control group, *TwGGPPS5* expression level in induced group showed a downward trend following MeJA treatment, eventually returning to control level at 72 h (Fig. S4). Phytochemical analysis revealed that triptolide accumulation statistically significant increased at 120 and 240 h ($p < 0.05$), reaching a maximum of 2.9-fold at 240 h compared with control group (Fig. S5). In order to analysis the correlation between the expression of genes and accumulation of triptolide, the relative (fold-induction) levels of three genes mRNA and accumulation of triptolide are exhibited in Fig. 6. The results showed that triptolide accumulation was enhanced concomitantly with the increased expression of *TwGGPPS1* and *TwGGPPS4*, which suggests that these two genes may be primarily responsible for triptolide synthesis.

A fuller understanding of the functions of GGPP synthases in plant isoprenoid networks will require comprehensive analyses combined with subcellular localisation studies. In this study, the TargetP1.1 server, PSORT and wolfpsort utilities were used to predict the subcellular localisation and identify signal peptides in the TwGGPPS sequences (Table 1). TwGGPPS1, which has a predicted chloroplast transit peptide (cTP) in its N-terminus, is likely an enzyme that uses IPP and DMAPP produced by the

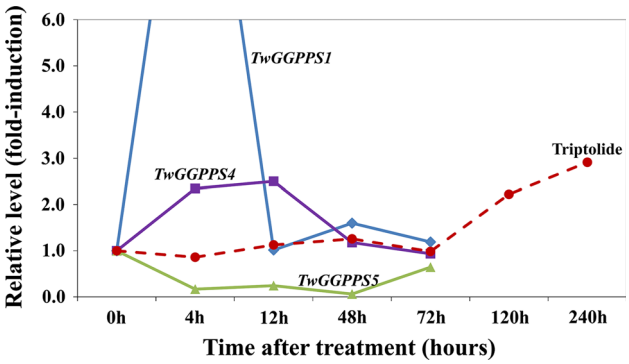

Fig. 6 Relative levels (fold-induction) of *TwGGPPS1* (*diamonds*), *TwGGPPS4* (*squares*), *TwGGPPS5* (*triangles*) and triptolide (*circles*) found in MeJA treated versus control suspension cell cultures of *T. wilfordii*

chloroplast MEP pathway as substrates. And it is primarily responsible for the synthesis of diterpenoids (Bick and Lange 2003), such as triptolide. TwGGPPS4 is likely localized to the cytoplasm, where it may catalyze the IPP produced through the MVA pathway, similar to the functions of GGPPS3 and GGPPS4 in *Arabidopsis thaliana* (Beck et al. 2013). Cytosolic GGPPSs are required for the production of substrates for the synthesis of cytosolic oligoprenols (ubiquinone, side chain, dolichols or diterpenoids), polyisoprenoids, and protein prenylation (Vranová et al. 2011). Therefore, in contrast to TwGGPPS4, TwGGPPS1 is likely the primary enzyme that mediates triptolide synthesis. TwGGPPS2 and TwGGPPS5 are likely located to the plasma membrane, and both belong to the type II GGPP synthase subfamily, having the GGPPS functional regions (FARM and SARM) and I–V conserved domains, but only TwGGPPS5 possesses the activity of GGPP synthase, it suggests that TwGGPPS2 may be a pseudogene. TwGGPPS3 and TwGGPPS6 are likely located to the chloroplast, both having no GGPPS activity. Some of TwGGPPS might have a physiological function rather than the role of being responsible for terpene biosynthesis. This study described six members of the GGPPS gene family in *T. wilfordii*. And three of these genes, *TwGGPPS1*, *TwGGPPS4* and *TwGGPPS5*, encode functional proteins. Correlation analyses of gene expression and secondary metabolite accumulation indicate that *TwGGPPS1* and *TwGGPPS4* may participate in triptolide biosynthesis. These findings lay the foundation for future studies on the biosynthetic pathways of triptolide and other diterpenoids in *T. wilfordii*.

Author contribution statement L.H, X.W and W.G designed the project, M.Z and P.S performed the research, and Y.Z, Y.L, Y.Z, Y.T and T.H participated in the research and analyzed the data; M.Z wrote the paper. All authors read and approved the final manuscript.

Acknowledgments This work was supported by the National Natural Science Foundation of China (81422053 and 81373906 to W.G, and 81325023 to L.H.), and National High Technology Research and Development Program of China (863 Program:2015AA0200908) to W.G., and the Author of National Excellent Doctoral Dissertation of China (201188) to W.G.

Compliance with ethical standards

Conflict of interest The authors declare no competing financial interest.

References

Ashby MN, Kutsunai SY, Ackerman S, Tzagoloff A, Edwards PA (1992) COQ2 is a candidate for the structural gene encoding parahydroxybenzoate: polyprenyltransferase. J Biol Chem 267:4128–4136

Beck G, Coman D, Herren E, Ruiz-Sola MA, Rodríguez-Concepción M, Gruissem W, Vranová E (2013) Characterization of the GGPP synthase gene family in *Arabidopsis thaliana*. Plant Mol Biol 82:393–416

Bick JA, Lange BM (2003) Metabolic cross talk between cytosolic and plastidial pathways of isoprenoid biosynthesis: unidirectional transport of intermediates across the chloroplast envelope membrane. Arch Biochem Biophys 415:146–154

Bouvier F, Rahier A, Camara B (2005) Biogenesis, molecular regulation and function of plant isoprenoids. Prog Lipid Res 44:357–429

Brinker AM, Ma J, Lipsky PE, Raskin I (2007) Medicinal chemistry and pharmacology of genus *Tripterygium* (Celastraceae). Phytochemistry 68:732–766

Del Sal G, Manfioletti G, Schneider C (1989) The CTAB-DNA precipitation method: a common mini-scale preparation of template DNA from phagemids, phages or plasmids suitable for sequencing. Biotechniques 7:514–520

Gao W, Hillwig ML, Huang L, Cui G, Wang X, Kong J, Yang B, Peters RJ (2009) A functional genomics approach to tanshinone biosynthesis provides stereochemical insights. Org Lett 11:5170–5173

Hemmi H, Noike M, Nakayama T, Nishino T (2003) Analternative mechanism of product chain-length determination in type III geranylgeranyl diphosphate synthase. Eur J Biochem 270:2186–2194

Huang J, Zhou L, Wu H, Pavlos N, Chim SM, Liu Q, Zhao J, Xue W, Tan RX, Ye J, Xu J, Ang ES, Feng H, Tickner J, Xu J, Ding Y (2015) Triptolide inhibits osteoclast formation, bone resorption, RANKL-mediated NF-κB activation and titanium particle-induced osteolysis in a mouse model. Mol Cell Endocrinol 399:346–353

Jiang X (1994) Clinical observations on the use of the Chinese herb *Tripterygium wilfordii* Hook for the treatment of nephrotic syndrome. Pediatr Nephrol 8:343–344

Joly A, Edward PA (1993) Effect of site-directed mutagenesis of conserved aspartate and arginine residues upon farnesyl diphosphate synthase activity. J Biol Chem 268:26983–26989

Kannaiyan R, Shanmugam MK, Sethi G (2011) Molecular targets of celastrol derived from Thunder of God Vine: potential role in the treatment of inflammatory disorders and cancer. Cancer Lett 303:9–20

Laule O, Fiirholz A, Chang HS (2003) Crosstalk between cytosolic and plastidial pathways of isoprenoid biosynthesis in *Arabidopsis thaliana*. Proc Natl Acad Sci USA 100:6866–6871

Li H, Zhang YY, Tan HW, Jia YF, Li D (2008) Therapeutic effect of tripterine on adjuvant arthritis in rats. J Ethnopharmacol 118:479–484

Li L, Li FQ, Wang XM (2010) Novel anti-inflammatory and neuroprotective agents for Parkinson's disease. CNS Neurol Disord Drug Targets 9:232–240

Liu J, Wu QL, Feng YH, Wang YF, Li XY, Zuo JP (2005) Triptolide suppresses CD80 and CD86 expressions and IL-12 production in THP-1 cells. Acta Pharmacol Sin 26:223–227

Liu Y, Tu S, Gao W, Wang Y, Liu P, Hu Y, Dong H (2013) Extracts of *Tripterygium wilfordii* Hook F in the treatment of rheumatoid arthritis: a systemic review and meta-analysis of randomised controlled trials. Evid Based Complement Alternat Med 2013:410793

Livak KJ, Schmittgen TD (2001) Analysis of relative gene expression data using real-time quantitative PCR and the $2^{-\Delta\Delta Ct}$ method. Methods 25:402–408

Memelink J, Verpoorte R, Kijne JW (2001) ORC Anization of jasmonate-responsive gene expression in alkaloid metabolism. Trends Plant Sci 6:212–219

Newman JD, Chappell J (1999) Isoprenoid biosynthesis in plant: carbon partitioning within the cytoplasmic pathway. Crit Rev Biochem Mol Biol 34:95–106

Patavino T, Brady DM (2001) Natural medicine and nutritional therapy as an alternative treatment in systemic lupus erythematosus. Altern Med Rev 6:460–471

Ren X, Zhang T, Hu J, Ding W, Wang X (2010) Triptolide T10 enhances AAV-mediated gene transfer in mice striatum. Neurosci Lett 479:187–191

Rohmer M, Knani M, Simonin P, Sutter B, Sahm H (1993) IsoPrenoid biosynthesis in bacteria: a novel pathway for the early steps leading to isopentenyl diphosphate. Biochem J 295:517–524

Song L, Poulter CD (1994) Yeast farnesyl-diphosphate synthase: site-directed mutagenesis of residues in highly conserved prenyltransferase domains I and II. Proc Natl Acad Sci USA 91:3044–3048

Su P, Cheng Q, Wang X, Cheng X, Zhang M, Tong Y, Li F, Gao W, Huang L (2014) Characterization of 8 terpenoids from tissue cultures of the Chinese herbal plant, *Tripterygium wilfordii*, by high-performance liquid chromatography coupled with electrospray ionization tandem mass spectrometry. Biomed Chromatogr 28:1183–1192

Titov DV, Gilman B, He QL, Bhat S, Low WK, Dang Y, Smeaton M, Demain AL, Miller PS, Kugel JF, Goodrich JA, Liu JO (2011) XPB, a subunit of TFIIH, is a target of the natural product triptolide. Nat Chem Biol 3:182–188

Vandermoten S, Haubruge E, Cusson M (2009) New insights into short-chain prenyltransferases: structural features, evolutionary history and potential for selective inhibition. Cell Mol Life Sci 66:3685–3695

Vranová E, Hirsch-Hoffmann M, Gruissem W (2011) AtIPD: a curated database of *Arabidopsis* isoprenoid pathway models and genes for isoprenoid network analysis. Plant Physiol 156:1655–1660

Wang GD, Dixon RA (2009) Heterodimeric geranyl(geranyl)diphosphate synthase from hop (*Humulus lupulus*) and the evolution of monoterpene biosynthesis. Proc Natl Acad Sci USA 106:9914–9919

Wang X, Liang XB, Li FQ, Zhou HF, Liu XY, Wang JJ, Wang XM (2008) Therapeutic strategies for Parkinson's disease: the ancient meets the future—traditional Chinese herbal medicine, electroacupuncture, gene therapy and stem cells. Neurochem Res 10:1956–1963

Yang S, Chen J, Guo Z, Xu XM, Wang L, Pei XF, Yang J, Underhill CB, Zhang L (2003) Triptolide inhibits the growth and metastasis of solid tumors. Mol Cancer Ther 2:65–72

Zhang M, Su P, Liu YJ, Tong YR, Zhao YJ, Gao W, Wang XJ, Huang LQ (2015) Cloning and bioinformatics analysis of geranylgeranyl diphosphate synthase gene of *Tripterygium wilfordii*. Chin J Chin Mater Med 40:1066–1070

Zhao YJ, Cheng QQ, Su P, Chen X, Wang XJ, Gao W, Huang LQ (2014) Research progress relating to the role of cytochrome P450 in the biosynthesis of terpenoids in medicinal plants. Appl Microbiol Biotechnol 98:2371–2383

Zhou YJ, Gao W, Rong Q, Jin G, Chu H, Liu W, Yang W, Zhu Z, Li G, Zhu G, Huang L, Zhao ZK (2012) Modular pathway engineering of diterpenoid synthases and the mevalonic acid pathway for miltiradiene production. J Am Chem Soc 134:3234–3241